Development and Validation of an Apoptosis-Related Genes Signature in Patients with Gastric Cancer

Jianqiao Yang
Shandong University Affiliated Hospital: Shandong Provincial Hospital
Liang Shang
Shandong University Affiliated Hospital: Shandong Provincial Hospital
Leping Li
Shandong University Affiliated Hospital: Shandong Provincial Hospital
Zixiao Wang
Shandong University School of Medicine: Shandong University Cheeloo College of Medicine
Kangdi Dong
Shandong University Affiliated Hospital: Shandong Provincial Hospital
Han Li (doclihan@126.com)
Shandong Qianfoshan Hospital https://orcid.org/0000-0002-3554-3991
Jin Liu
Shandong University Affiliated Hospital: Shandong Provincial Hospital

Research Article

Keywords: Gastric cancer, apoptosis-related genes, prognostic biomarkers, Immunohistochemical, Nomogram

Posted Date: December 15th, 2021

DOI: https://doi.org/10.21203/rs.3.rs-1099716/v1

Abstract

Background: Gastric cancer (GC) is a common malignant tumour of the digestive tract. the prognosis of GC patients is still not optimistic. Apoptosis-related genes (ARGs) plays an important role in the development, invasion, metastasis and drug resistance of GC. Therefore, assessing the interaction between ARGs and the prognosis of GC patients may help identify specific biomarkers.

Methods: Differentially expressed genes (DEGs) were identified by integrating gene expression profiling analyses from The Cancer Genome Atlas (TCGA) GC cohort and Gene Set Enrichment Analysis (GSEA) Database. Then, a risk score model was built based on Kaplan-Meier (K-M), least absolute shrinkage and selector operation (LASSO), and multivariate Cox regression analyses. Another cohort (GSE84426) was used for external validation. By combining risk scores with clinical variables, a nomogram was constructed to predict the prognosis of GC patients.

Results: We screened 39 DEGS and established a three-gene signature(CAV1□F2□LUM) based on 161 ARGs. In addition, three-gene signature was identified as an independent factor in predicting the prognosis of GC patients and validated in an external independent cohort. Finally, we developed a nomogram that can be applied to clinical practice.

Conclusions: Our study established a three-gene signature of GC based on ARGs that has reference significance for in-depth research on the apoptosis mechanism of GC and the exploration of new clinical treatment strategies.

Introduction

Gastric cancer (GC) is a malignant gastrointestinal tumour that seriously threatens human health, and its morbidity and mortality rank fifth and third among malignant tumours, respectively[1,2]. As GC patients are often diagnosed at an advanced stage, the long-term prognosis of patients is not ideal[3]. In addition, surgical treatment and first-line chemotherapy with platinum-containing drugs are still the main choice for treatment of GC, but the efficacy of the above treatment methods in advanced GC has reached a bottleneck; therefore, novel treatment methods are urgently needed[4,5]. In recent years, with the rise of second-generation sequencing technology, the expression regulation mechanism of some special types of genes has been clarified. By combining gene expression profiles with clinical information from patients, some biomarkers with predictive value for patient prognosis have been obtained[6,7]. Early diagnosis, prognosis prediction and even identification of potential therapeutic targets can be realized through these biomarkers. However, due to the lack of specificity and sensitivity, only a few prognostic markers of GC are applicable to clinical practice.

Apoptosis, also known as programmed cell death, is an effective mechanism to actively remove ageing or damaged cells in the process of growth and development[8]. Apoptosis is highly regulated by apoptosis-related genes (ARGs) and involves multiple signaling pathway. Triggering of apoptosis depends on

caspase-mediated internal pathway, external pathways or endoplasmic reticulum pathway, which ultimately lead to morphological and biochemical changes in cells[9]. Usually, the proliferation and apoptosis of cells maintain a dynamic balance. Once the mechanism of apoptosis is altered, this balance is broken, promoting the occurrence and development of tumours[10–12]. Preliminary studies on the relationship between apoptosis and GC showed that the expression products of ARGs could be independent factors influencing the poor prognosis of GC patients[13]. In addition, some studies have shown that a targeted drug not only plays an anticancer role through anti-angiogenesis, but also inhibits tumour progression by inducing apoptosis-related genes and inhibiting the expression of anti-apoptotic genes[14].

Given the existing findings, we know that apoptosis-related genes are closely related to the occurrence and development of GC. However, comprehensive and systematic research is still lacking. In this study, We established a three-genes signature and Nomogram to predict the prognosis of GC patients, and preliminarily revealed their complex biological functions and involved signaling pathways related to ARGs, aiming to provide guidance for individualized prediction and treatment of patients with GC.

Materials And Methods

Acquisition of apoptosis-related genes

The Molecular Signatures Database (version 7.4) (http://software.broadinstitute.org/gsea/msigdb) of the GSEA database (http://software.broadinstitute.org/gsea/index.jsp) was used to download the "HALLMARK_APOPTOSIS" gene sets, and ARGs were obtained in total. For details, please see Table S1.

Collection of RNA sequencing data and clinical information

RNA-seq data from 343 GC samples and 30 normal samples were obtained from the TCGA database (https://cancergenome.nih.gov/). In addition, we downloaded the clinical information of 365 GC patients with a survival time over 30 days from the database. At the same time, RNA-seq data and clinical information of the external validation cohort (n=76) were downloaded from the GEO database (https://www.ncbi.nlm.nih.gov/geo/, ID:GSE84426). All gene expression-related data were normalized by log2 transformation, and all patients with incomplete clinical data were excluded.

Relationship between apoptosis-related genes and prognosis of gastric cancer

We selected | log2FC | > 1, FDR < 0.05 as the critical value, and the "limma" package was used to determine differentially expressed apoptosis-related genes. The “ClusterProfiler” package was used for Gene Ontology (GO) enrichment analysis and Kyoto Encyclopedia of Genes and Genomes (KEGG) pathway analysis of differentially expressed genes. The Search Tool for the Retrieval of Interacting Genes (STRING)database was used (Version 11.5) (http://www.string-db.org/) to construct the PPI between differentially expressed genes, and the results were visualized by Cytoscape software.

Identification of a three-gene signature

Univariate Cox regression analysis was performed to identify the ARGs related to the prognosis of GC patients, and the cut-off p value was set to 0.05. The least absolute shrinkage and selection operator (LASSO)Cox regression model (“glmnet” package) was used to narrow down the candidate genes and establish the prognostic model. The penalty parameter (λ) was determined by the minimum criterion, and the three ARGs and their coefficients were obtained. Three ARG expression levels in normal and GC tissues ("limma "package) were compared, and the Human Protein Atlas (HPA) database (http://www.proteinatlas.org/) was used to compare the 3 gene expression levels at the protein level. The samples were divided into a high expression group (n=152) and a low expression group (n=153), with the median expression level of the three genes as the critical value. The "survivor" package was used to analyse survival differences between the high expression group and the low expression group. Finally, the cBioPortal database (http://cbioportal.org) was used to analyse the gene mutations of these 3 genes.

Development of the apoptosis-related gene prognostic model

By combining the expression levels and risk coefficients of the 3 ARGs, a risk score formula was established: Risk Score = $\Sigma 3\ iX_i \times Y_i$ (X: coefficient, Y: gene expression level). After calculating the risk score for each GC patient, the patients were divided into high-risk and low-risk groups at the median risk score cut-off. The "survminer" package was used to draw Kaplan–Meier survival curves and describe the survival distribution of the patients. Finally, the "time-ROC" package was used to draw receiver operating characteristic (ROC) curves, and the area under the curve (AUC) value was calculated to evaluate the predictive power and accuracy of the prognostic model.

Independent prognostic analysis of the risk score

The risk score and other clinical variables (age, gender, grade, T stage, N stage, and M stage) were included in the univariate and multivariate Cox regression analyses (cut-off p value:0.05) to determine the independent prognostic factors of GC patients.

External validation of the GEO cohort

According to the risk score formula obtained from the TCGA cohort, the risk score of patients in the GEO dataset GSE84426 was calculated. Patients were divided into high-risk and low-risk groups using the median risk score as the cut-off value. Kaplan–Meier survival curves and ROC curves were drawn to evaluate the predictive power of the prognostic model in an external independent cohort.

Construction of a nomogram to predict the prognosis of gastric cancer patients

The forward stepwise selection method for optimizing AIC applied based on multivariate Cox analysis was used to identify variables, and the “rms” package was used to integrate them to construct a

nomogram for predicting the prognosis of GC patients. Meanwhile, 1-year, 3-year, and 5-year calibration curves and the C-index were used to assess the accuracy of the nomogram.

Statistical analysis

Single-factor analysis of variance was used to compare gene expression levels between GC samples and normal samples. Kaplan–Meier survival analysis with a two-sided log-rank test was used to compare the outcomes of patients in different groups. Univariate and multivariate Cox regression were used to analyse the independent prognostic values of the variables. All statistical analyses were accomplished with R software (v4.0.2). The overall flow diagram is shown in Fig. 9.

Results

Identification of differentially expressed apoptosis-related genes

We identified 39 differentially expressed genes(DEGs)between normal tissues and GC tissues. There were 26 up-regulated genes (CASP8, LUM, IFITM3, CCND1, SLC20A1, BIK, CDK2, TAP1, TNFRSF12A, KRT18, BID, EREG, PMAIP1, CASP2, LEF1, PDGFRB, AIFM3, BRCA1, CDC25B, PLPPR4, TIMP1, F2R, ERBB2, TOP2A, BGN, and F2) and 13 down-regulated genes (BTG2, GPX3, GADD45B, IGFBP6, RHOB, GSN, TGFBR3, GSTM1, CAV1, DCN, JUN, CDKN1A, and TXNIP). The expression distribution of DEGs is presented in Fig. 1A-C.

Functional enrichment analysis and protein interaction network

To determine the main biological function of the DEGs and the pathways involved, GO enrichment analysis and KEGG pathway analysis were performed on 39 DEGs. The results of GO enrichment analysis showed that the main biological pathways of DEG enrichment were the extrinsic apoptotic signaling pathway and positive regulation of the cell cycle. The main enriched cell components were the cycle-dependent protein kinase holoenzyme complex and lysosomal lumen. The main enriched molecular function was ubiquitin/ubiquitin-like protein ligase binding (Fig. 2A, B). In addition, KEGG pathway analysis showed that these genes were not only highly enriched in apoptotic pathways, but also involved in the regulation of the p53/PI3K-Akt signaling pathway, platinum drug resistance, Epstein-Barr virus infection and some carcinogenic pathways (Figure 2C, 2D). To further explore the interactions between these ARGs, we PPI analysis using the STRING database and visualized the results using Cytoscape. We finally identified 36 apoptotic genes as hub genes. Among them, 23 genes were up-regulated and 13 genes were down-regulated (Figure 2E).

Association between ARGs and gastric cancer patient survival and prognosis

After univariate Cox regression analysis, we obtained 10 ARGs associated with the prognosis of GC patients ($P < 0.05$). Among them, 9 genes (CAV1, DCN, F2, F2R, GADD45B, GPX3, IGFBP6, LUM, and PDGFRB) were negatively correlated with the prognosis of GC patients, and one gene (TAP1) was positively correlated with prognosis (Figure 3A). By performing LASSO Cox regression analysis, a 3-gene signature (CAV1, LUM and F2) was constructed according to the optimum λ value (Fig. 3B, C). By comparing the RNA expression and protein expression levels of 3 ARGs between GC tissues and normal tissues, we found that the expression levels of the 3 ARGs in GC samples were significantly increased compared with those in normal samples (Fig. 3D). To further analyse the correlation between the expression of 3 ARG genes and the prognosis of GC patients, we divided the samples into a high expression group (n=152) and a low expression group (n=153) using the median expression level of genes as the critical value. Kaplan–Meier analysis showed that the survival rate of the high expression group was significantly lower than that of the low expression group (Figure 3E). Gene mutations in 3 ARGs were analysed using the cBioPorta database (Figure 3F). A total of 434 patients were enrolled, of whom 46 (11%) had a genetic mutation. Among the 3 ARGs, F2 was the most prone to mutation (5%), while LUM was the gene with the lowest mutation probability but the greatest number of possible mutations (missense mutation, truncating mutation, amplification and deep deletion).

We further compared the expression differences of the 3 ARGs at the protein level between GC and normal tissues. Immunohistochemical results showed that the expression of CAV1, F2 and LUM at the protein level in gastric cancer tissues was higher than that in normal tissues (Fig. 4), which was consistent with our previous results and further verified the prognostic value of the three genes.

Establishment of a prognostic risk signature based on apoptosis-related genes

By combining the expression levels of 3 ARGs with the risk coefficient, the prognostic risk score formula of GC patients was established. Risk score= (0.1457×expression levels of CAV1) + (0.2978×expression levels of F2) + (0.1317×expression levels of LUM). After calculating the risk score of each patient according to the above formula, patients were divided into a high-risk group (n=152) and a low-risk group (n=153) using the median risk score as the critical value (Fig. 5A). The survival distribution of patients (Figure 5B) showed that patients in the high-risk group had more deaths and shorter survival times than those in the low-risk group. Kaplan–Meier (K-M) analysis showed a statistically significant difference in survival between the high-risk and low-risk groups ($P < 0.0001$) (Figure 5C). The survival rate of the high-risk group was significantly lower than that of the low-risk group, especially in regards to 2- and 3-year survival rates. A ROC curve showed that the prognostic model had good sensitivity and specificity, and the AUC values of the 1-year, 3-year and 5-year survival rates were 0.630, 0.657 and 0.722, respectively (Figure 5D).

Independent prognostic value of the risk model

To determine whether the risk score was an independent predictor of prognosis in patients with GC ($P < 0.05$), univariate and multivariate Cox regression analyses were performed to compare the risk score and

other clinical prognostic variables. The results of univariate Cox regression analysis (Fig. 6A) showed that age, tumour stage, N stage and risk score were correlated with the prognosis of GC patients. Multivariate Cox regression analysis showed that risk score (P < 0.001) and age (P=0.001) were independent predictors of the prognosis of GC patients (Fig. 6B). In addition, ROC curves were used to verify the accuracy of each factor in predicting the prognosis of GC patients. Comparison of the AUC values of each curve, showed that the AUC value of the risk score (AUC=0.631) was significantly higher than that of the clinical variables, indicating that the risk score had higher predictive power and accuracy than the clinical variables (Fig. 6C).

External validation of the risk signature

The risk score of patients in the GEO dataset GSE84426 (n=76) was calculated by the previously established risk scoring formula. According to the median risk score, patients were divided into high-risk (n=38) and low-risk groups (n=38). GSEA was used to identify differences between the high- and low-risk groups stratified by the apoptosis-related signature. The results showed that ECM receptor interaction, the calcium signaling pathway, and focal adhesion were significantly enriched in the high-risk group (Fig. 7A). K-M survival analysis showed that patients in the high-risk group of the external independent cohort also had significantly lower outcomes than those in the low-risk group (P=0.018) (Fig. 7B). The AUC values of the ROC curve (1-year, 3-year and 5-year survival rates: 0.579, 0.605 and 0.650, respectively) further verified the high accuracy of the risk score (Fig. 7C).

Development of a prognostic nomogram

To apply the risk score to clinical practice, we integrated risk scores with clinical variables to construct a nomogram to predict the prognosis of GC patients. The forward stepwise selection method for optimizing AIC applied based on multivariate Cox analysis was used to ultimately identify two variables, risk score and age. According to the actual situation of each patient, the corresponding score of each factor was obtained, and the 1-year, 3-year and 5-year survival rates of the patient were calculated after obtaining total score (Fig. 8A). The results showed that higher final scores were correlated with shorter survival times. Furthermore, the calibration curves for 1-year, 3-year and 5-year survival rates were used to verify the prediction ability of the line graph, and the results showed that the predicted value was in strong agreement with the actual value (C index =0.607) (Fig. 8B-D).

Discussion

Apoptosis, also known as programmed cell death, plays an important role in the human body as a homeostasis and defence mechanism[15]. Unlike necrosis, apoptosis is an active process that is highly regulated by genes. Typically, when cells in precancerous lesions have irreparable DNA damage, the body activates apoptosis to remove potentially harmful cells and prevent tumour growth. Therefore, maladjustment of the apoptosis mechanism is considered to be closely related to the occurrence and development of tumours and drug resistance to tumour therapy[16,17], but it also provides clues for the development of new therapeutic methods.

In this study, 38 ARGs with differential expression in GC samples and normal samples were identified. GO enrichment analysis and KEGG bypass analysis showed that most DEGs were involved in the regulation of the cell cycle, the external signaling pathway of apoptosis, the p53/PI3K-Akt signaling pathway, etc. To further evaluate the relationship between ARGs and the prognosis of GC patients, we constructed a 3-gene risk model by univariate Cox regression analysis and LASSO Cox regression analysis. According to the median risk score, patients were divided into a high-risk group and a low-risk group, and the survival rate of the high-risk group was significantly lower than that of the low-risk group. In addition, multivariate Cox analysis showed that the risk model was an independent factor in predicting the prognosis of GC patients, and the independent cohort of the GEO database further verified that the model had high prognostic ability for GC patients. To further apply the risk model in practice, we constructed a nomogram for predicting the prognosis of GC patients.

In our study, three ARGs (CAV1, LUM, and F2) were identified as potential therapeutic targets for GC, all of which were highly expressed in GC tissues and were negatively correlated with the prognosis of GC patients. The CAV1 expression product caeolin-1 is a carcinogenic membrane protein associated with endocytosis, signal transduction and lipid metabolism disorders[18]. Previous studies have shown that CAV1 can both promote and inhibit tumour development, possibly dependent on tumour type and stage. On the one hand, CAV1 can play an inhibitory role in cancer by promoting cell cycle arrest and preventing cell transformation[19–21]. On the other hand, the CAV1 gene can promote cancer by inhibiting apoptosis and promoting tumour metastasis and drug resistance[22,23]. Previous studies have shown that high expression of CAV1 is positively correlated with disease progression and poor prognosis of GC patients[24,25], which is consistent with our findings (HR value of CAV1 < 1). Some studies have explored the possible mechanism by which CAV1 affects the prognosis of GC patients. On the one hand, CAV1 can enhance the receptor activator of nuclear factor-κB (RANK) pathway leading to GC cell migration [26]. On the other hand, Caeolin-1 promotes cisplatin resistance in GC cells by activating the WNT/β-catenin pathway[27]. The expression product of the LUM gene is a type of proteoglycan in the extracellular matrix, which is involved in receptor-mediated signal transduction and affects tumour proliferation[28]. Similar to the CAV1 gene, the LUM gene can both promote and inhibit tumour proliferation[29]. Compared with surrounding normal tissues, the LUM gene is highly expressed in GC tissues[30] and is positively correlated with increased tumour invasiveness and poor prognosis[31], both of which were verified in our study. Studies have shown that the LUM gene can be involved in the occurrence and metastasis of GC by activating the integrin β1-FAK signaling pathway[32]. The F2 gene encodes prothrombin protein, which is hydrolysed multiple times to form active thrombin. In addition to its functions of thrombosis and haemostasis, thrombin plays an important role in cell proliferation and tumour angiogenesis [33,34]. Scholars have explored the correlation between F2 and cancer[35,36], and mutation of F2 was proven to be associated with an increased prevalence of gastrointestinal tumours[37]. In vitro animal experiments have shown that prothrombin can promote tumour growth, invasion and metastasis by acting on PAR-1 and fibrin in colon cancer[38]. At present, there are no reports to clarify the role of F2 in the occurrence and development of GC. Our study showed that F2 was highly expressed in GC tissues with a high mutation

probability and was negatively correlated with the prognosis of GC patients, which may provide clues for subsequent studies.

In conclusion, our study confirms that ARGs are associated with poor prognosis in patients with GC. In addition, we established a risk score model based on ARGs, which was verified by an independent external cohort with high predictive efficacy. We also established a nomogram combining risk score and age, which further improves the practicability of the risk model in clinical application and improves the sensitivity of individualized survival prediction for GC patients.

Abbreviations

ARGs: apoptosis-related genes; TCGA: The Cancer Genome Atlas; GSEA: Gene Set Enrichment Analysis: GEO: Gene Expression Omnibus; DEGs differentially expressed genes; GO: Gene Ontology; KEGG: Kyoto Encyclopedia of Genes and Gnomes; STRING: The Search Tool for the Retrieval of Interacting Genes; PPI: Protein-Protein Interaction Network; LASSO: the least absolute shrinkage and selection operator; HPA: Human Protein Atlas.

Declarations

Acknowledgements

We would like to acknowledge the TCGA, GSEA and the GEO (GSE84426) network for providing data.

Author contributions

J.L conceived and designed the study. L.L revised the manuscript and make final approval of the version. Y.J analyzed data and wrote the manuscript. Z.W and K.D reviewed the data, H.L and L.S interpretated results and helped to write the manuscript.

Funding

This study was supported by Key Research and Development Program of Shandong Province(2019JZZY010104); Special Foundation for Taishan Scholars Program of Shandong Province(ts20190978); and Science and Technology Innovation Development Program of Jinan (2020019082).

Availability of data and materials

The data could be download at (https://portal.gdc.cancer.gov/,http://www.gsea-msigdb.org/gsea/index.jsp, andhttps://www.ncbi.nlm.nih.gov/geo/; GSE84426) and the code used during the current study are available from the corresponding author on reasonable request.

Ethics approval and consent to participate

Not applicable.

Consent for publication

Not applicable.

Competing interests

The authors declare that they have no competing interests.

References

1. Van Cutsem E, Sagaert X, Topal B, Haustermans K & Prenen H. Gastric cancer. Lancet. 2016,388:2654-2664.
2. Ferlay J, Colombet M, Soerjomataram I, Mathers C, Parkin DM, Piñeros M, et al. Estimating the global cancer incidence and mortality in 2018: GLOBOCAN sources and methods. Int J Cancer. 2019,144,1941-1953.
3. Gupta GP & Massagué J. Cancer metastasis: building a framework. Cell. 2006,127,679-95.
4. Ford HE, Marshall A, Bridgewater JA, Janowitz T, Coxon FY, Wadsley J, et al. Docetaxel versus active symptom control for refractory oesophagogastric adenocarcinoma (COUGAR-02): an open-label, phase 3 randomised controlled trial. Lancet Oncol. 2014,15,78-86.
5. Kang JH, Lee SI, Lim DH, Park KW, Oh SY, Kwon HC, et al. Salvage chemotherapy for pretreated gastric cancer: a randomized phase III trial comparing chemotherapy plus best supportive care with best supportive care alone. J Clin Oncol. 2012,30,1513-8.
6. Li Z, Yang AJ, Wei FM, Zhao XH & Shao ZY. Significant association of DIRC1 overexpression with tumor progression and poor prognosis in gastric cancer. Eur Rev Med Pharmacol Sci. 2018,22,8682-8689.
7. Ishiwata T. Role of fibroblast growth factor receptor-2 splicing in normal and cancer cells. Front Biosci. 2018,23:626-639.
8. Fuchs Y & Steller H. Programmed cell death in animal development and disease. Cell. 2011,147,742-58.
9. Wong RS. Apoptosis in cancer: from pathogenesis to treatment. J Exp Clin Cancer Res. 2011,30,87.
10. Correa P & Piazuelo MB. The gastric precancerous cascade. J Dig Dis. 2012,13,2-9.
11. Brenes F, Ruiz B, Correa P, Hunter F, Rhamakrishnan T, Fontham E, et al. Helicobacter pylori causes hyperproliferation of the gastric epithelium: pre- and post-eradication indices of proliferating cell nuclear antigen. Am J Gastroenterol. 1993,88,1870-5.
12. Scotiniotis IA, Rokkas T, Furth EE, Rigas B & Shiff SJ. Altered gastric epithelial cell kinetics in Helicobacter pylori-associated intestinal metaplasia: implications for gastric carcinogenesis. Int J Cancer. 2000,85,192-200.

13. Kim MA, Lee HE, Lee HS, Yang HK & Kim WH. Expression of apoptosis-related proteins and its clinical implication in surgically resected gastric carcinoma. Virchows Arch. 2011,459,503-10.
14. Jia X, Wen Z, Sun Q, Zhao X, Yang H, Shi X, et al. Apatinib suppresses the Proliferation and Apoptosis of Gastric Cancer Cells via the PI3K/Akt Signaling Pathway. J BUON. 2019,24,1985-1991.
15. Fuchs Y & Steller H. Programmed cell death in animal development and disease. Cell. 2011,147,742-758.
16. Plati J, Bucur O & Khosravi-Far R. Dysregulation of apoptotic signaling in cancer: molecular mechanisms and therapeutic opportunities. J Cell Biochem. 2008,104,1124-1149.
17. Fulda S. Tumor resistance to apoptosis. Int J Cancer. 2009,124,511-515.
18. Sotgia F, Martinez-Outschoorn UE, Howell A, Pestell RG, Pavlides S & Lisanti MP. Caveolin-1 and cancer metabolism in the tumor microenvironment: markers, models, and mechanisms. Annu Rev Pathol. 2012, 7,423-467.
19. Galbiati F, Volonte D, Engelman JA, Watanabe G, Burk R, Pestell RG, et al. P. Targeted downregulation of caveolin-1 is sufficient to drive cell transformation and hyperactivate the p42/44 MAP kinase cascade. The EMBO journal. 1998,17, 6633–6648 .
20. Rimessi A, Marchi S, Patergnani S & Pinton P. H-Ras-driven tumoral maintenance is sustained through caveolin-1-dependent alterations in calcium signaling. Oncogene. 2014,33,2329-2340.
21. Volonte D, Zhang K, Lisanti MP & Galbiati F. Expression of caveolin-1 induces premature cellular senescence in primary cultures of murine fibroblasts. Mol Biol Cell. 2002,13,2502-2517.
22. Patani N, Martin LA, Reis-Filho JS & Dowsett M. The role of caveolin-1 in human breast cancer. Breast Cancer Res Treat. 2012,131,1-15.
23. Nwosu ZC, Ebert MP, Dooley S & Meyer C. Caveolin-1 in the regulation of cell metabolism: a cancer perspective. Mol Cancer. 2016,15,71.
24. Seker M, Aydin D, Bilici A, Yavuzer D, Ozgun MG, Ozcelik M, et al. Correlation of Caveolin-1 Expression with Prognosis in Patients with Gastric Cancer after Gastrectomy. Oncol Res Treat. 2017,40,185-190.
25. Nam KH, Lee BL, Park JH, Kim J, Han N, Lee HE, Kim MA, Lee HS, Kim WH. Caveolin 1 expression correlates with poor prognosis and focal adhesion kinase expression in gastric cancer. Pathobiology. 2013,80,87-94.
26. Wang Y, Song Y, Che X, Zhang L, Wang Q, Zhang X, et al. Caveolin-1 enhances RANKL-induced gastric cancer cell migration. Oncol Rep. 2018,40,1287-1296.
27. Wang X, Lu B, Dai C, Fu Y, Hao K, Zhao B, et al. Caveolin-1 Promotes Chemoresistance of Gastric Cancer Cells to Cisplatin by Activating WNT/β-Catenin Pathway. Front Oncol. 2020,10,46.
28. Chen S & Birk DE. The regulatory roles of small leucine-rich proteoglycans in extracellular matrix assembly. FEBS J. 2013,280,2120-2137.
29. Appunni S, Anand V, Khandelwal M, Gupta N, Rubens M & Sharma A. Small Leucine Rich Proteoglycans (decorin, biglycan and lumican) in cancer. Clin Chim Acta. 2019,491,1-7.

30. Chen X, Li X, Hu X, Jiang F, Shen Y, Xu R, et al. LUM Expression and Its Prognostic Significance in Gastric Cancer. Front Oncol. 2020, 10,605.
31. Chen L, Zhang Y, Zuo Y, Ma F & Song H. Lumican expression in gastric cancer and its association with biological behavior and prognosis. Oncol Lett. 2017,14,5235-5240.
32. Wang X, Zhou Q, Yu Z, Wu X, Chen X, Li J, et al. Cancer-associated fibroblast-derived Lumican promotes gastric cancer progression via the integrin β1-FAK signaling pathway. Int J Cancer. 2017,141,998-1010.
33. Trikha M & Nakada MT. Platelets and cancer: implications for antiangiogenic therapy. Semin Thromb Hemost. 2002,28,39-44.
34. Ma YY, He XJ, Wang HJ, Xia YJ, Wang SL, Ye ZY, et al. Interaction of coagulation factors and tumor-associated macrophages mediates migration and invasion of gastric cancer. Cancer Sci. 2011,102,336-42.
35. Vairaktaris E, Yapijakis C, Wiltfang J, Ries J, Vylliotis A, Derka S, Vasiliou S, Neukam FW. Are factor V and prothrombin mutations associated with increased risk of oral cancer? Anticancer Res. 2005,25,2561-5.
36. Ghasemi S, Tavakoli A, Moghadam M, Zargar MA, Abbaspour M, Hatamnejadian N, et al. Risk of prostate cancer and thrombosis-related factor polymorphisms. Biomed Rep. 2014,2,53-56.
37. Pihusch R, Danzl G, Scholz M, Harich D, Pihusch M, Lohse P, et al. Impact of thrombophilic gene mutations on thrombosis risk in patients with gastrointestinal carcinoma. Cancer. 2002,94,3120-6.
38. Adams GN, Rosenfeldt L, Frederick M, Miller W, Waltz D, Kombrinck K, et al. Colon Cancer Growth and Dissemination Relies upon Thrombin, Stromal PAR-1, and Fibrinogen. Cancer Res. 2015,75,4235-43.

Figures

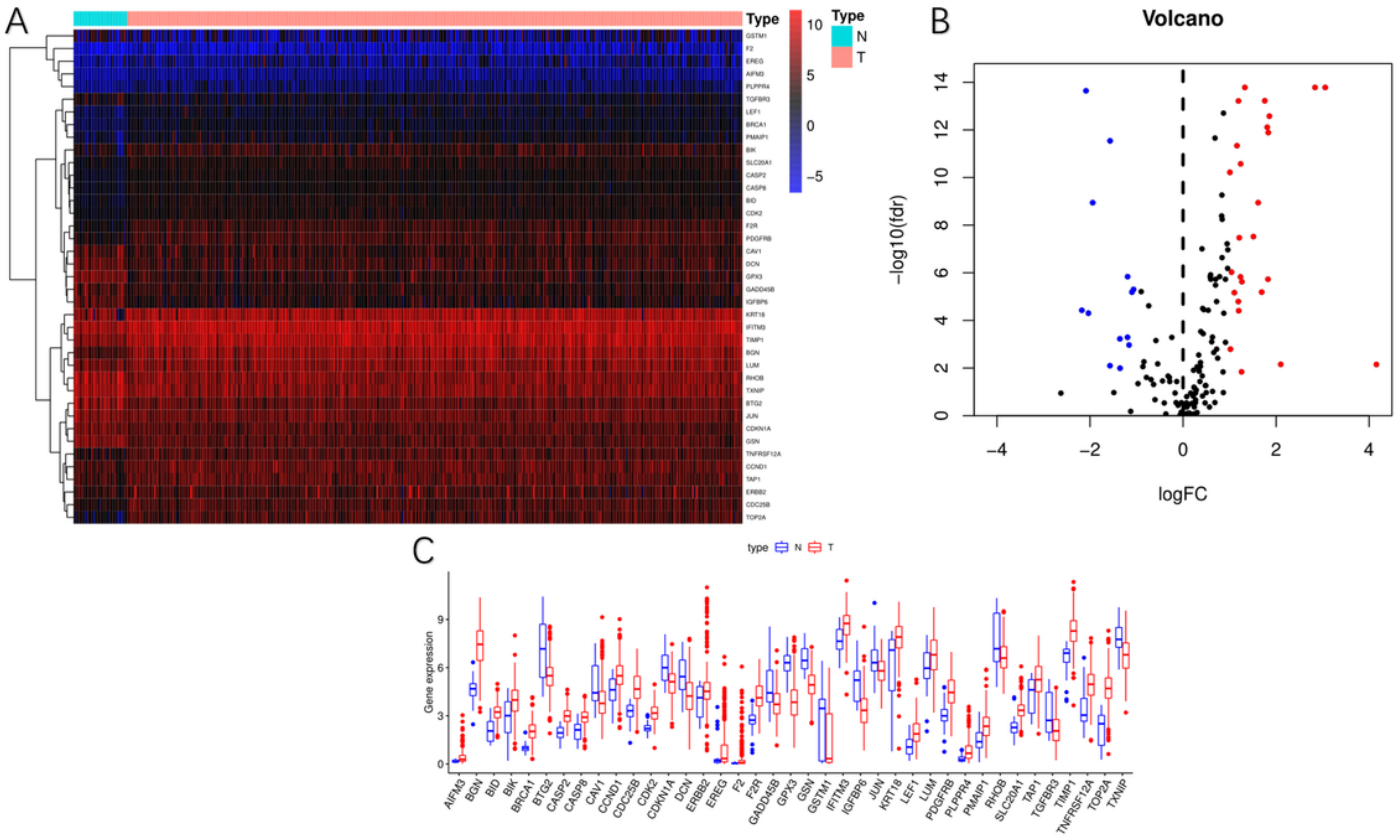

Figure 1

The differentially expressed ARGs. A The heatmaps of 39 differentially expressed ARGs. B The boxplot of the differentially expressed ARGs. (Red represents high expression, blue represents low expression, black represents no difference between HCC and normal tissues.) C The volcano plot of the differentially expressed ARGs (N indicates non-tumor tissues; T indicates tumor tissues).

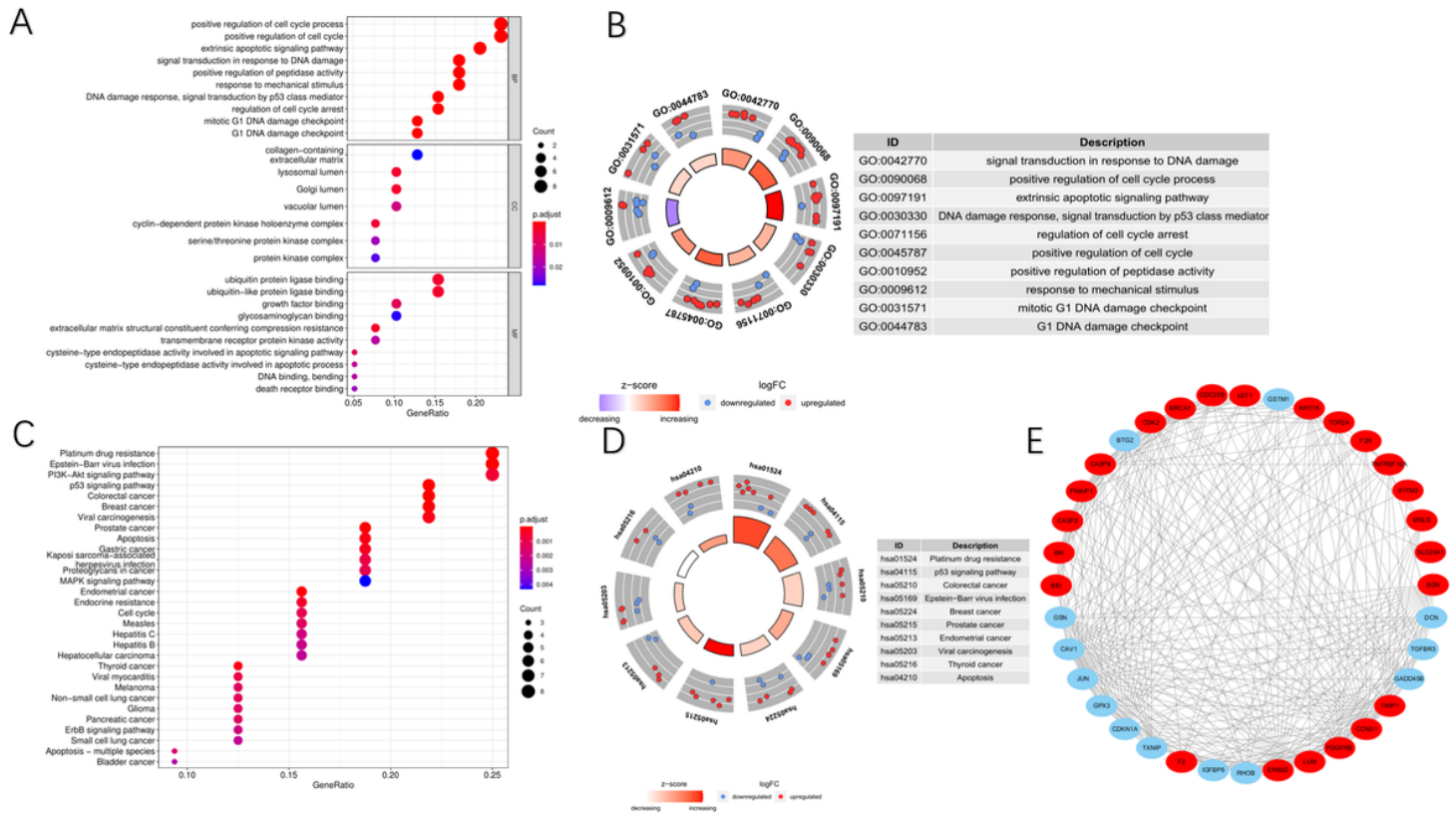

ID	Description
GO:0042770	signal transduction in response to DNA damage
GO:0090068	positive regulation of cell cycle process
GO:0097191	extrinsic apoptotic signaling pathway
GO:0030330	DNA damage response, signal transduction by p53 class mediator
GO:0071156	regulation of cell cycle arrest
GO:0045787	positive regulation of cell cycle
GO:0010952	positive regulation of peptidase activity
GO:0009612	response to mechanical stimulus
GO:0031571	mitotic G1 DNA damage checkpoint
GO:0044783	G1 DNA damage checkpoint

ID	Description
hsa01524	Platinum drug resistance
hsa04115	p53 signaling pathway
hsa05210	Colorectal cancer
hsa05169	Epstein-Barr virus infection
hsa05224	Breast cancer
hsa05215	Prostate cancer
hsa05213	Endometrial cancer
hsa05203	Viral carcinogenesis
hsa05216	Thyroid cancer
hsa04210	Apoptosis

Figure 2

GO and KEGG analysis of differentially expressed ARGs. A–C The top 30 significant terms of GO function enrichment and KEGG analysis. BP biological process, CC cellular component, MF molecular function. B–D The GO circle and the KEGG circle shows the scatter map of the logFC of the specified gene. (The larger the circle, the greater the number of enrichment; The redder the color, the higher the significance of enrichment; The higher the Z-score value indicated, the higher expression of the enriched pathway). E The correlation network of the ARGs (Red represents up-regulation, bule represents down-regulation).

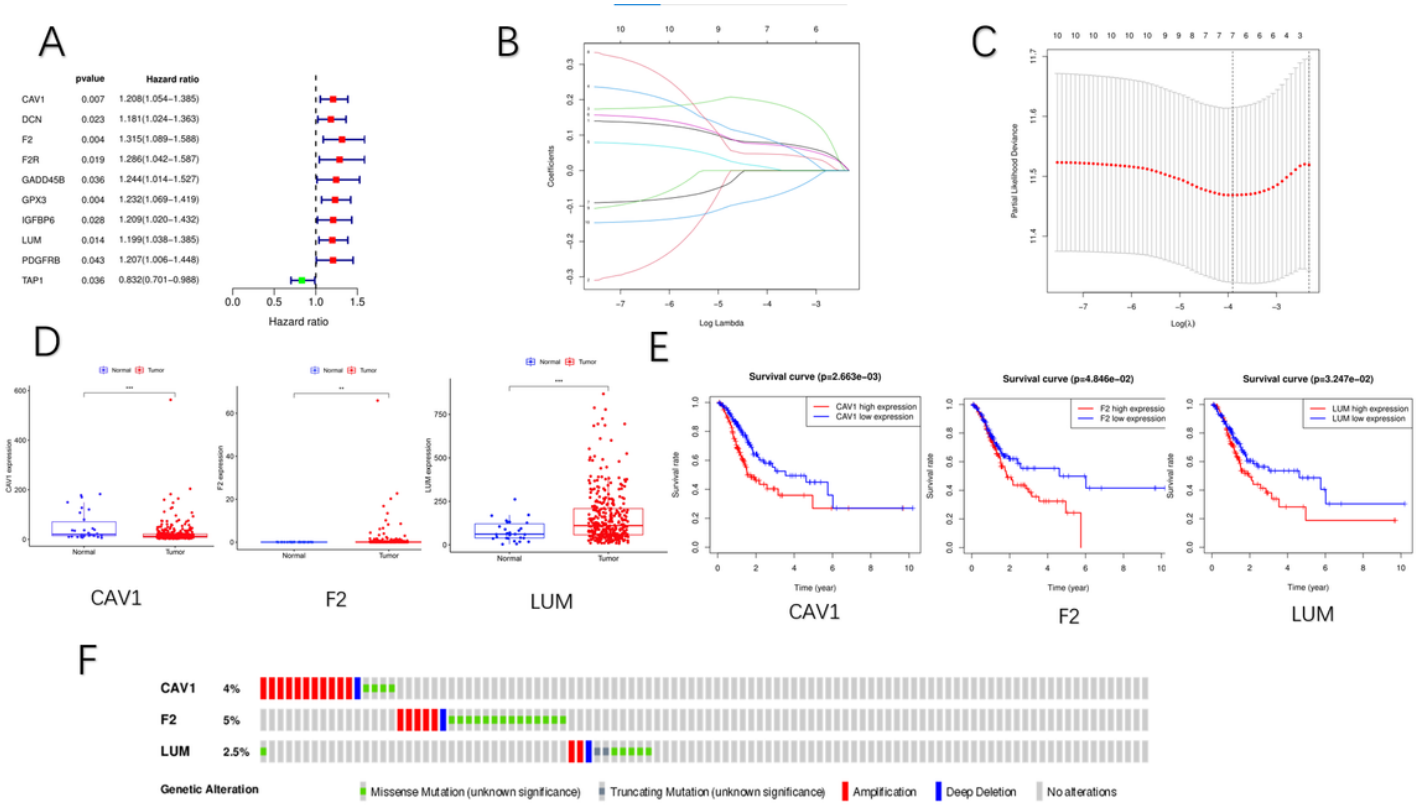

Figure 3

Identification of ARGs associated with the prognosis of GC. A The forest plot of univariate Cox regression results; B LASSO regression of the 10 OS-related genes; C Cross-validation for tuning the parameter selection in the LASSO regression; D Expression levels of 3 screened ARGs in GC and normal samples. E KM curve of the relationship between OS in GC patients and expression levels of 3 screened ARGs. F Mutation data of 3 screened ARGs among 434 GC specimens.

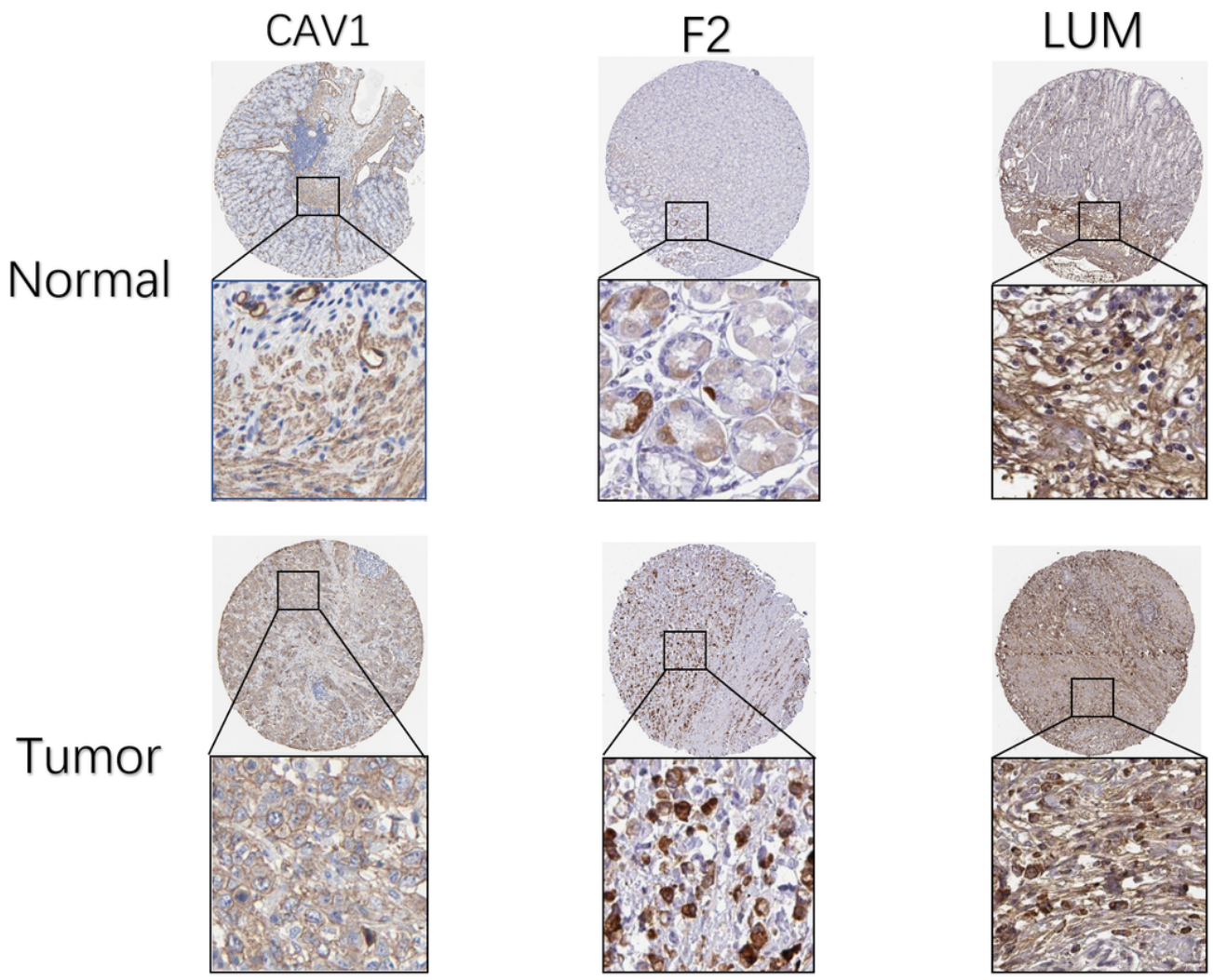

Figure 4

Immunohistochemical results of the expression levels of 3 screened ARGs between GC and para-carcinoma tissues according to the Human Protein Atlas (HPA) database;

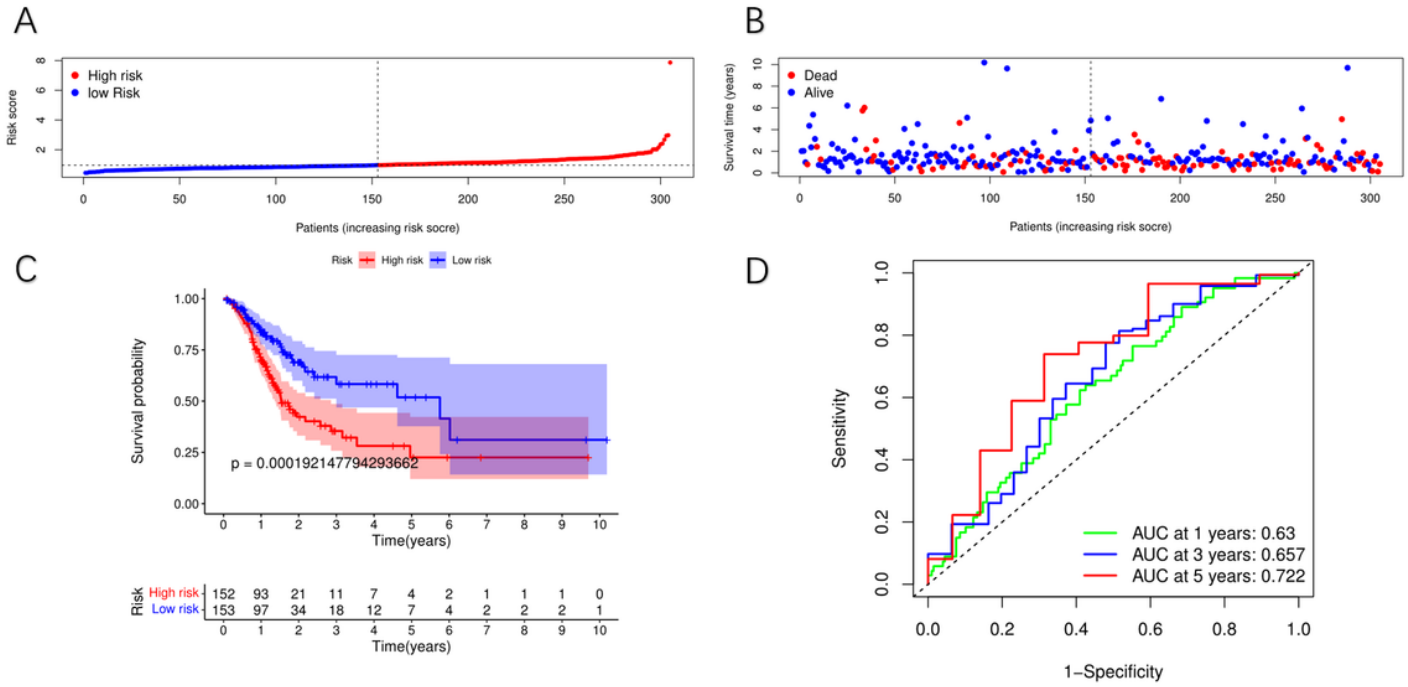

Figure 5

Construction of risk signature in the TCGA cohort. A Distribution of patients based on the risk score. B The survival status for each patient (low-risk population: on the left side of the dotted line; high-risk population: on the right side of the dotted line). C Kaplan–Meier curves for the OS of patients in the high- and low-risk groups. D ROC curves demonstrated the predictive efficiency of the risk score.

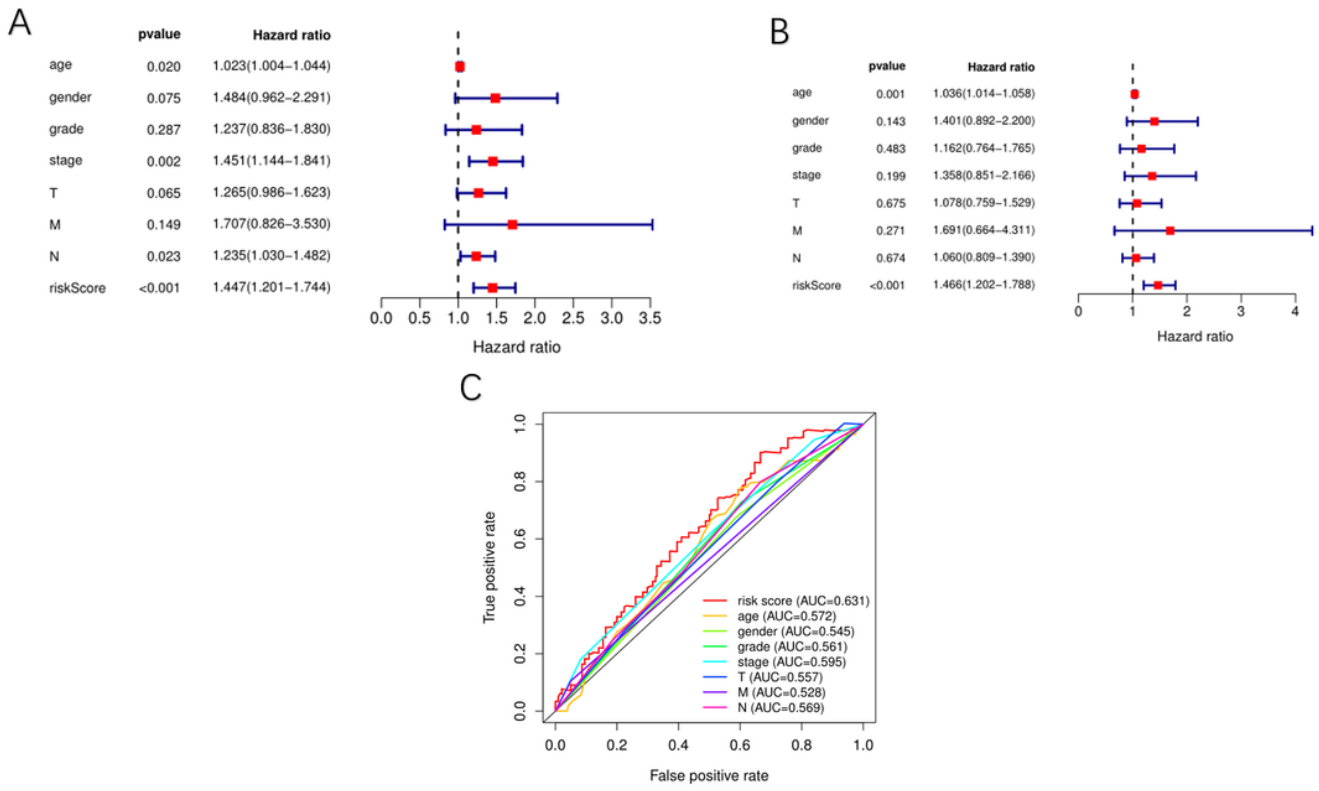

Figure 6

Prognostic effect analysis of risk score and clinical features in GC. A univariate Cox regression analysis for the TCGA cohort. B multivariate Cox regression analysis for the TCGA cohort. C The ROC analysis of the risk score and other prognostic clinical features in GC.

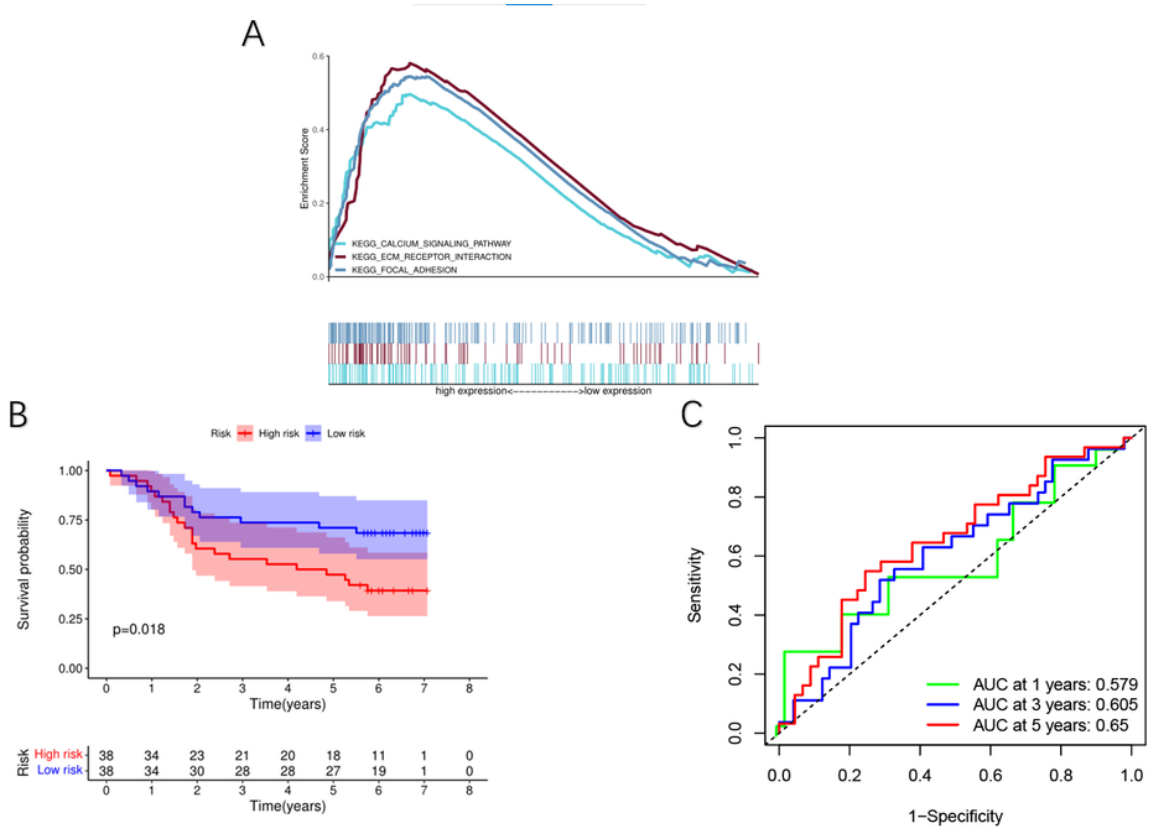

Figure 7

Validation of the apoptosis -related signature in GEO dataset. A GSEA analyzed e differences between high- and low-risk groups stratified by the apoptosis-related signature. B Kaplan–Meier curves of OS in the high-risk and the low-risk groups stratified by the apoptosis -related signature in the GSE84426. C The ROC analysis in the GSE84426.

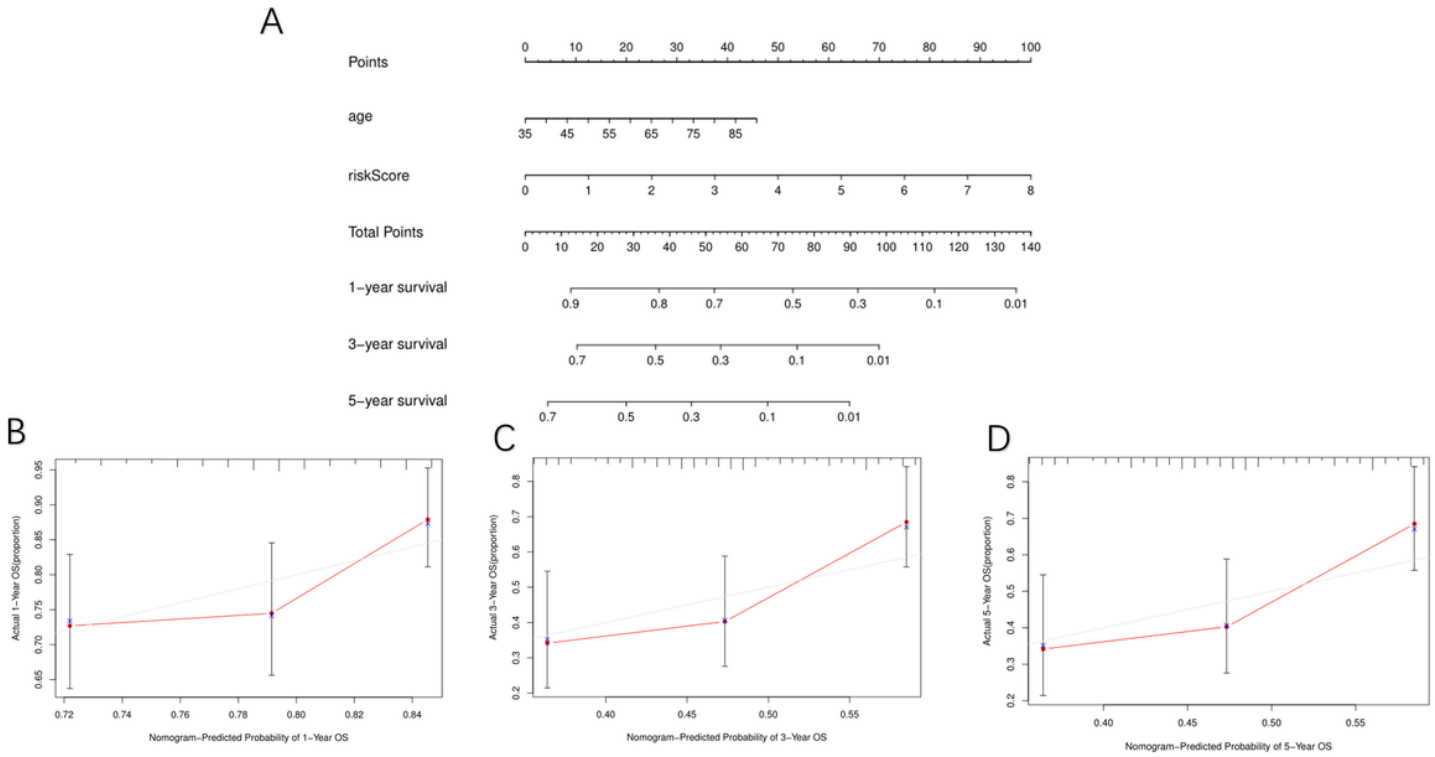

Figure 8

Nomogram considering apoptosis-related signature and clinical factors for prediction of the individualized survival probability of GC patients. A Development of a nomogram containing age and risk score to predict 1-, 3-, and 5-year OS. B–D Calibration plots of the nomograms in terms of the agreement between nomogram-predicted and observed 1-, 3-, and 5-year survival outcomes of the GC cohort. The 45◦dashed line represents the ideal performance. The actual performances of the model are represented by the red lines, and the figures from left to right illustrate the 1-, 3-, and 5-year results, respectively.

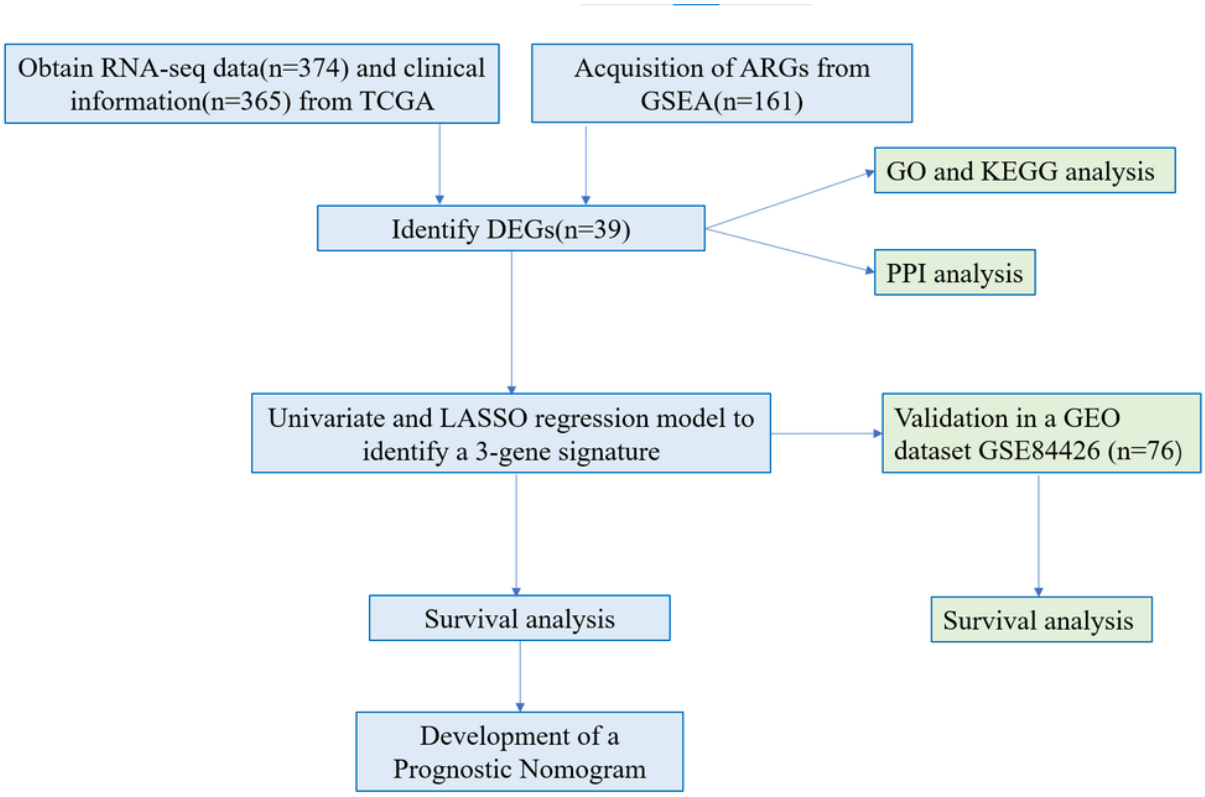

Figure 9

Workflow diagram. The specific workflow graph of data analysis.

Supplementary Files

This is a list of supplementary files associated with this preprint. Click to download.

- Supplementarytable1.docx
- Supplementarytable2.docx
- Supplementarytable3.docx